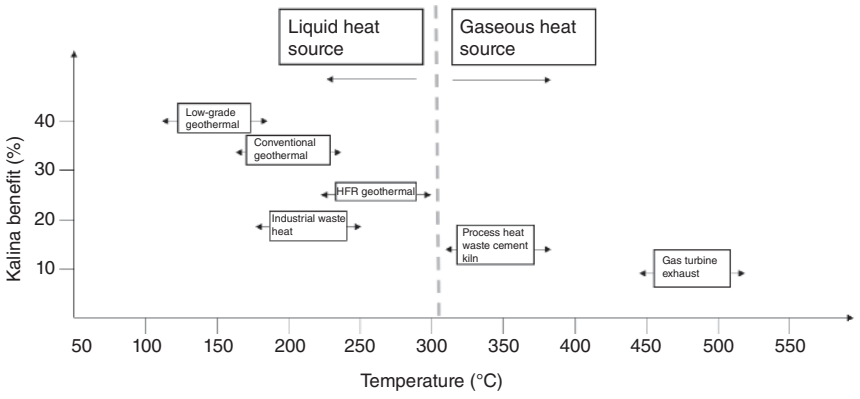

Figure 1.49 Kalina benefit as a function of heat temperature and types of applications.

1.4.3.1 The Different Configurations of the Cycle

Kalina cycles are part of a thermodynamic family of cycles. These vary by the number of each component, how they are arranged, and how they are linked together. To date, a lot of interesting Kalina cycle configurations have been designed and studied; every configuration being suitable for a particular type of application and so designated by a code. For example, KCS-1 was the very first cycle that used a mixture of fluids and was proposed by Kalina himself in 1984 [42].

All these thermodynamic cycles are split into two groups. The oldest ones are called *first-generation* Kalina cycles – the Kalina cycle being a trademark involving all the first-generation Kalina cycles [43].

Figure 1.50 shows three configurations of the Kalina cycle system [44], all suitable for geothermal applications. KCS-11 was designed for the high-temperature geothermal resources and KCS-34 for lower temperature geothermal resources. Those two cycles are the most common Kalina cycles used for geothermal application. KSG-1 is very similar to KCS-34, the KSG-1 patent is held by Siemens.

A second generation of Kalina cycle was developed by Dr. Alexander Kalina from 2008 to 2014. The patents for those new cycles are all owned by a company called Kalex LLC, founded by Kalina.

Those new cycles are more efficient and provide an improved power output. For example, the SG-2a cycle offers a better energetic and exergetic efficiency than either KCS-11 or KCS-34 when using geothermal heat sources in temperature range from 125 to 150 °C [45].

So even though these new cycles have a more complex architecture than their first-generation counterparts and so are consequently more expensive, they still offer a shorter payback period [46]. Second-generation Kalina cycles therefore seem most promising, and configurations now exist for biomass, geothermal, solar thermal, cement waste heat, bottoming cycle, and ocean solar thermal applications [47].

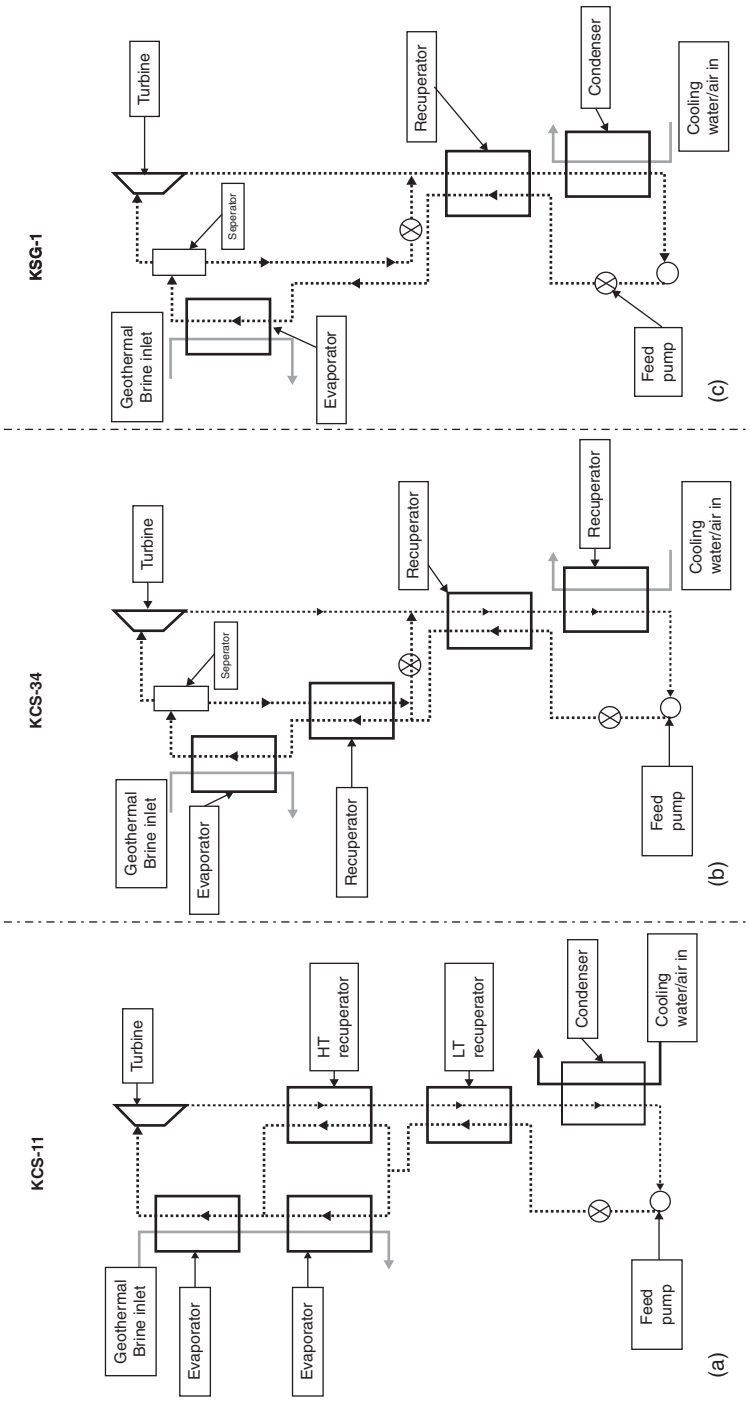

Figure 1.50 (a–c) Schematic of different Kalina cycle systems [44]. Source: Wang and Yu [44].

Table 1.4 Kalina cycle case studies from around the world [39].

Name	Country	Commissioned	Output (MW)	Heat sources
Canoga Park	USA	1992	6.5	Nuclear waste heat
Fukuoka	Japan	1998	4	Waste incineration
Sumitomo Metals	Japan	1999	3.5	Waste heat
Husavik	Iceland	2000	2	Geothermal
Fuji Oil	Japan	2005	3.9	Waste heat
Bruschal	Germany	2009	0.6	Geothermal
Unterhaching	Germany	2009	3.5	Geothermal
Shanghai Expo	China	2010	0.05	Solar hot water
Quingshui	Taiwan	2011	0.05	Geothermal

Source: Global cement [39].

1.4.4 Case Studies

Some pilot power plants exist and are currently producing energy using Kalina cycles. Table 1.4 lists case studies from around the world as of 2012.

The first large-scale Kalina cycle-based power plant was built in the United States in 1992 and operated for five years recovering nuclear waste heat and was able to produce 6.5 MW of electricity [39].

A famous Kalina-based plant (KCS-34) was built in Húsavík, Iceland. It is a 2 MW geothermal power plant and harnesses the energy of 125 °C geothermal brine, providing 80% of the electrical demand of the local town's 2500 inhabitants [48]. Another geothermal power plant (KCS34), also harnessing geothermal hot brine through a Kalina cycle, is located at Unterhachting in Germany. This power plant is generating 3.4 MW of electricity. The geothermal brine is also providing 38 MW of thermal energy to a district heating system. A third geothermal power plant (KCS-34) using the Kalina technology is the Bruchsal power plant [49], also in Germany.

Further Kalina cycle projects had been designed since 2012. For example, the Star Cement plant in Dubai is a 4.75 MW plant also using this technology [3], and it is anticipated, as we move forward, that more and more projects utilising Kalina cycles technology will evolve [50].

1.5 Brayton Cycle

The Brayton cycle is also known as the 'gas turbine cycle' or the *Joule* cycle. It is an open cycle, whereby the intake and exhaust points are both open to the environment [51].

Air enters the engine and is compressed by the compressor (resulting in HP air). Energy is then added by spraying fuel into the air and igniting it within the combustion chamber, and now this high-temperature pressurised gas is used to drive a turbine (mounted on the same shaft as the compressor) to produce work output. Finally, the combusted gases and any unused energy leaves through the exhaust and in doing so some of this unused energy can be recovered.

First though, the Brayton cycle itself. This consists of a compression stage (process 1–2) which takes place adiabatically followed by a second stage (process 2–3) – the heat addition process – which occurs isobarically. The third stage (process 3–4) is an expansion process which occurs adiabatically and the final stage (process 4–1), heat rejection, occurs isobarically, all as shown in Figure 1.51.

The Brayton cycle is different from the Otto and Diesel cycles in that the processes occur within an open system. Therefore, in order to determine the heat transfer and work for the process an open system and steady flow analysis are used.

The schematic of the open Brayton process is shown in Figure 1.52, however, to further define the process as a cycle we need to include the heat output as shown in Figure 1.53.

The thermal efficiency of the Brayton η_{th} cycle is given by the following equation:

$$\eta_{th} = \frac{W_{net}}{Q_{in}} = 1 - \frac{Q_{out}}{Q_{in}} \tag{1.69}$$

where W_{net} (kJ) is the net work output of the system, Q_{in} (kJ) is the heat input, and Q_{out} (kJ) is the heat output.

The conservation of mass then gives:

$$\dot{m}_{in} = \dot{m}_{out} \tag{1.70}$$

$$\dot{m}_2 = \dot{m}_3 = \dot{m} \tag{1.71}$$

where m_2 and m_3 are the mass flow rate of fluid leaving the compressor and the mass flow rate entering the turbine (kg/s), respectively.

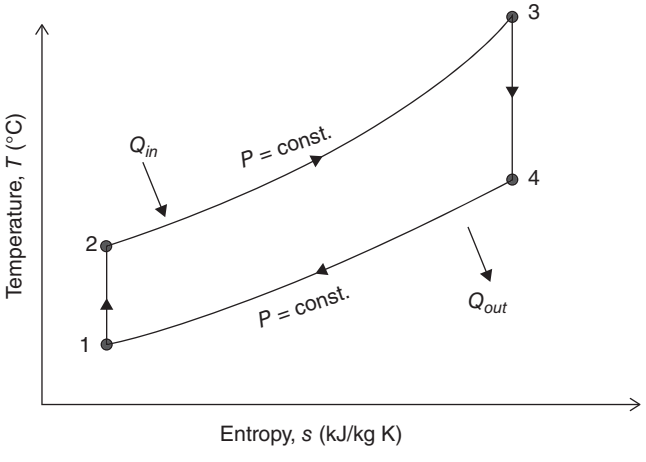

Figure 1.51 Temperature entropy graph for a Brayton cycle.

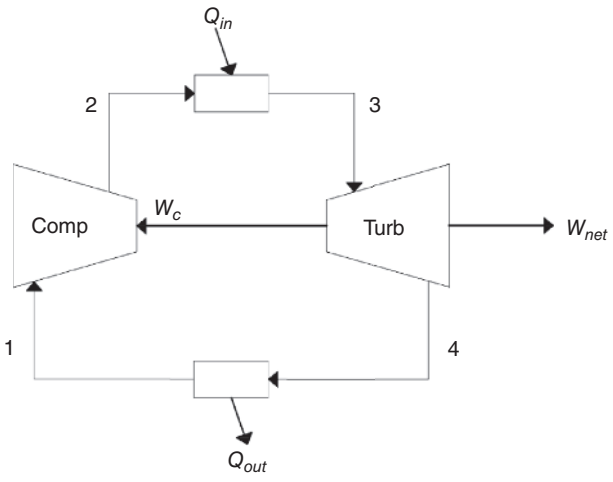

Figure 1.52 Gas turbine engine.

Figure 1.53 Closed Brayton cycle.

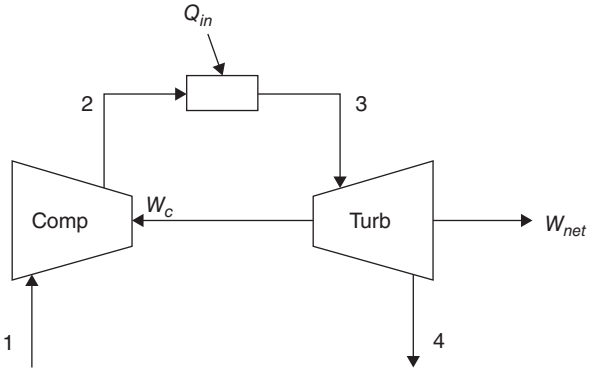

Therefore,

$$\eta_{th} = 1 - \frac{q_{out}}{q_{in}} = 1 - \frac{C_p(T_4 - T_1)}{C_p(T_3 - T_2)} \tag{1.72}$$

where $q_{out}(\text{kJ/kg}) = \frac{Q_{out}}{m}$, C_p (kJ/kg K) is the specific heat capacity of the working fluid (depending on the temperature), and T_x (K) is the temperature of the fluid given point.

Assuming the specific heat is constant (cold air standard analysis) gives:

$$\eta_{th} = 1 - \frac{T_4 - T_1}{T_3 - T_2} = 1 - \frac{T_1\left(\frac{T_4}{T_1} - 1\right)}{T_2\left(\frac{T_3}{T_2} - 1\right)} \tag{1.73}$$

And as processes 1–2 and 3–4 are isentropic:

$$\frac{T_2}{T_1} = \left(\frac{P_2}{P_1}\right)^{\frac{k-1}{k}} \tag{1.74}$$

$$\frac{T_3}{T_4} = \left(\frac{P_3}{P_4}\right)^{\frac{k-1}{k}} \tag{1.75}$$

In these last two equations, k is the heat capacity ratio, also known as the adiabatic index.

Moreover, as processes 2–3 and 4–1 are isobaric:

$$P_2 = P_3 \tag{1.76}$$

$$P_4 = P_1 \tag{1.77}$$

Thus,

$$\frac{T_2}{T_1} = \frac{T_3}{T_4} \tag{1.78}$$

Which can also be written this way:

$$\frac{T_4}{T_1} = \frac{T_3}{T_2} \tag{1.79}$$

So that finally, the efficiency of the ideal Brayton cycle is given by:

$$\eta_{th} = 1 - \frac{T_1}{T_2} \tag{1.80}$$

Now as the pressure ratio is defined as:

$$r_p = \frac{P_2}{P_1} \tag{1.81}$$

Figure 1.54 shows a typical pressure ratio curve for gas turbine engine.

Then the efficiency of the cycle can also be written using this coefficient as:

$$\eta_{th} = 1 - \frac{1}{r_p^{\frac{k-1}{k}}} \tag{1.82}$$

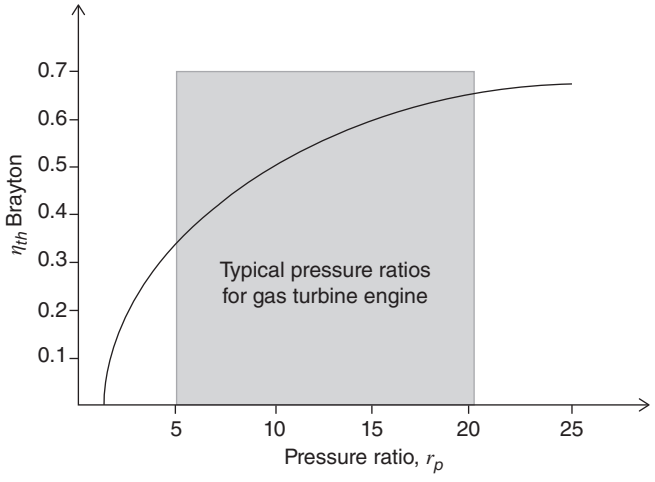

Figure 1.54 Typical pressure ratios for a gas turbine engine.

However, this is not the whole of the story because some of work produced by the turbine is also used by the compressor, the amount given back being defined by the back-work ratio (*BWR*) from:

$$BWR = \frac{W_{in}}{W_{out}} = \frac{W_{comp}}{W_{turb}} \tag{1.83}$$

1.5.1 Regenerative Brayton Cycle (Regenerator)

Because the temperature of the turbine exhaust is higher than the exit stream of the compressor, it presents an ideal opportunity to install a heat exchanger located between the hot exhaust of the turbine and the cooler gas leaving the compressor. Such a heat exchanger is also known as a regenerator or a recuperator. Figure 1.55 shows a schematic of the regenerative Brayton cycle.

And so in describing the efficiency of this regenerator, a *regenerator efficiency* term needs to be introduced, its calculation involving $q_{regen,max}$ and $q_{regen,act}$,and which can be obtained through enthalpy differences expressed in kJ/kg (see Figure 1.56).

$$\varepsilon_{regen} = \frac{q_{regen,max}\,(\text{kJ/kg})}{q_{regen,act}\,(\text{kJ/kg})} \tag{1.84}$$

$$q_{regen,max} = h_5' - h_2 = h_4 - h_2 \tag{1.85}$$

$$q_{regen,act} = h_5 - h_2 \tag{1.86}$$

Hence,

$$\varepsilon_{regen} = \frac{h_5 - h_2}{h_4 - h_2} \tag{1.87}$$

For ideal gases using the cold air standard analysis with constant specific heat, the regenerator effectiveness becomes:

$$\varepsilon_{regen} = \frac{T_5 - T_2}{T_4 - T_2} \tag{1.88}$$

So, for the efficiency of the cycle (using the closed cycle analysis) this leads to:

$$\eta_{th,regen} = 1 - \frac{q_{out}}{q_{in}} = 1 - \frac{h_6 - h_1}{h_3 - h_5} \tag{1.89}$$

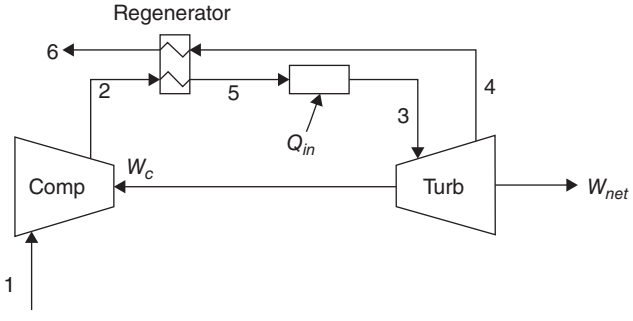

Figure 1.55 Schematic of the regenerative Brayton cycle.

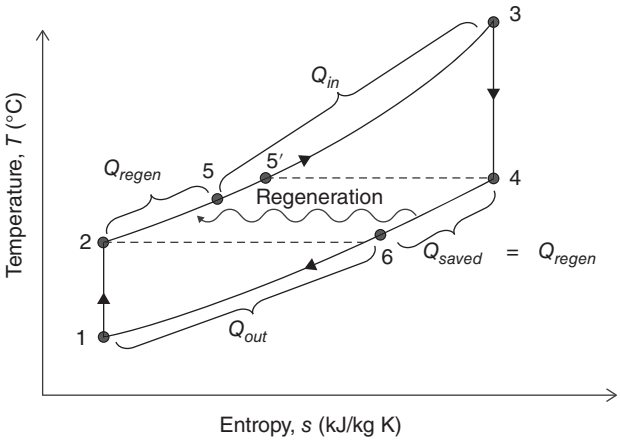

Figure 1.56 Temperature entropy graph for a regenerative Brayton cycle.

And assuming the efficiency of the regenerator is equal to 1, this then gives:

$$\eta_{th,regen} = 1 - \frac{T_1}{T_3} r_p^{\frac{k-1}{k}} \tag{1.90}$$

Figure 1.56 shows the temperature entropy profile for a regenerative Brayton cycle.

1.5.1.1 Compressor Analysis

The work (kW) used by the compressor is given by the following equation:

$$\dot{W}_{act,comp} = \dot{m}(h_{2a} - h_1) \tag{1.91}$$

where $\dot{m}$ is the mass flow rate of working fluid (in kg/s) and h_x is the enthalpy at the given point (kJ/kg).

Hence the adiabatic efficiency of the compressor is given by:

$$\eta_{comp} = \frac{\dot{W}_{isen,comp}}{\dot{W}_{act,comp}} = \frac{h_{2s} - h_1}{h_{2a} - h_1} \cong \frac{T_{2s} - T_1}{T_{2a} - T_1} \tag{1.92}$$

And the isentropic temperature at the outlet of the compressor is given by:

$$T_{2s} = T_1 \left(\frac{P_2}{P_1} \right)^{\frac{k-1}{k}} \tag{1.93}$$

1.5.1.2 Turbine Analysis

The work provided by the turbine (kW) is given by the following equation:

$$\dot{W}_{act,turb} = \dot{m}(h_3 - h_{4a}) \tag{1.94}$$

From which, the adiabatic efficiency of the turbine is given by:

$$\eta_{turb} = \frac{\dot{W}_{act,turb}}{\dot{W}_{isen,turb}} = \frac{h_3 - h_{4a}}{h_3 - h_{4s}} \cong \frac{T_3 - T_{4a}}{T_3 - T_{4s}} \tag{1.95}$$

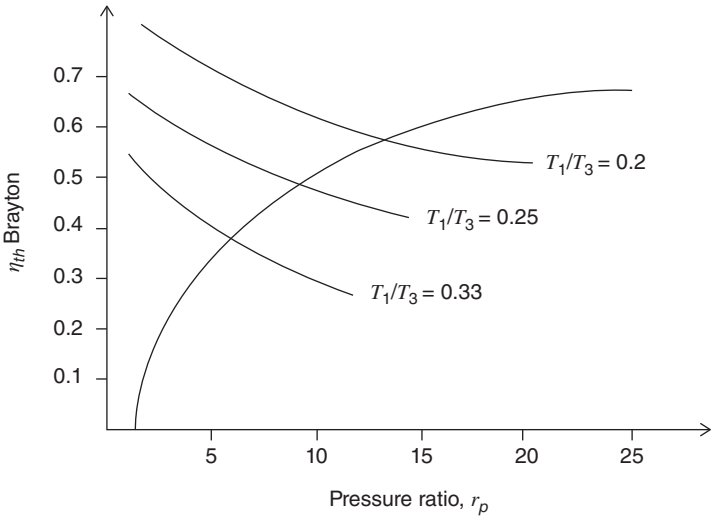

Figure 1.57 Regenerative Brayton cycle efficiency as a function of the pressure ratio and minimum and maximum temperature ratio.

And so, the isentropic temperature at the outlet of the turbine is given by:

$$T_{4s} = T_3\left(\frac{P_4}{P_3}\right)^{\frac{k-1}{k}} \tag{1.96}$$

1.5.1.3 Heat Supplied to the Cycle

The heat supplied to the cycle (kJ/kg) for process 5 to 3 can be calculated as follows:

$$q_{in} = h_3 - h_5 = C_p(T_3 - T_5) \tag{1.97}$$

The plot in Figure 1.57 shows the regenerative Brayton cycle efficiency as a function of the pressure ratio and minimum and maximum temperature ratio, T_1/T_3.

Thus, when the efficiency of the regenerative cycle is equal to the standard Brayton cycle then:

$$r_p = \left(\frac{T_3}{T_1}\right)^{\frac{k}{2(k-1)}} \tag{1.98}$$

1.5.2 Regenerative Brayton Cycle (Reheater and Intercooler)

The performance of a Brayton cycle can be further improved by incorporating an intercooler and a reheat process, the process schematic in Figure 1.58 shows a potential layout for a Brayton cycle with such additions. The concept is simple. During multi-stage compression, cooling the working fluid between each stage ultimately reduces the amount of work that is required by each compressor. This is because if we reduce the specific volume of the working fluid by cooling, then less work is required to achieve a set pressure increase.

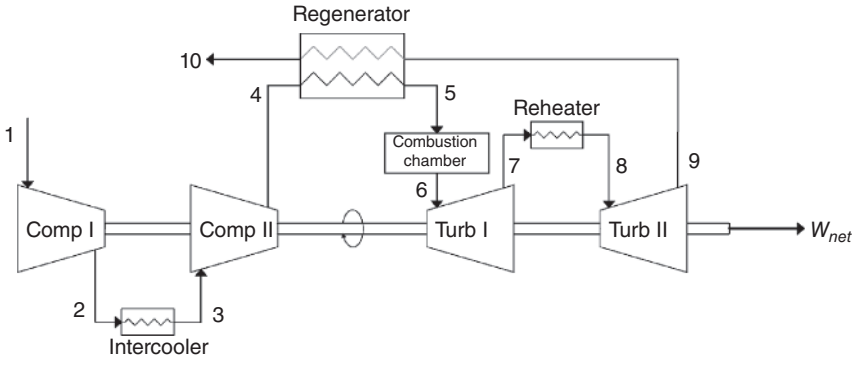

Figure 1.58 Schematic of the regenerative Brayton cycle with intercooler and reheat.

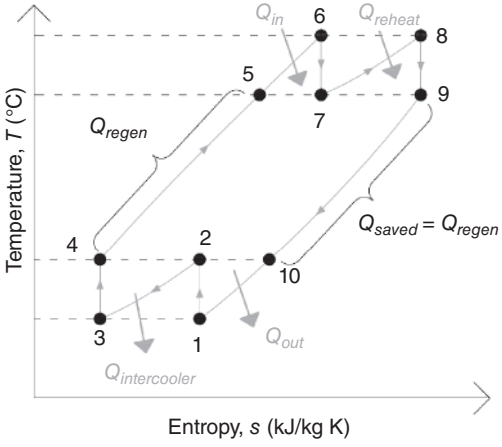

Figure 1.59 Temperature entropy graph for a regenerative Brayton cycle with a reheater and an intercooler.

So, incorporating a reheating process between two or more turbines of a multi-stage expansion ultimately results in an increase in the net work done and therefore a more efficient cycle. The temperature against entropy for this thermodynamic cycle is shown in Figure 1.59.

1.5.2.1 Intercooling

To minimise the work used by the compressors, P_2 (Pa) should be set as:

$$P_2 = \sqrt{P_1 P_4} \tag{1.99}$$

As the process 2–3 is isobaric, it can also be written as follows:

$$\frac{P_2}{P_1} = \frac{P_4}{P_2} = \frac{P_4}{P_3} \tag{1.100}$$

1.5.2.2 Reheating

To maximise the turbine work, P_7 should be set as:

$$P_7 = \sqrt{P_6 P_9} \tag{1.101}$$

As the process 7–8 is isobaric, it can also be written this way:

$$\frac{P_6}{P_7} = \frac{P_7}{P_9} = \frac{P_8}{P_9} \tag{1.102}$$

1.6 Chapter Summary

To conclude, the Rankine cycle can be considered (alongside the Carnot cycle) as the basis for all the external combustion thermodynamic cycles that aim to convert thermal energy into mechanical energy. In most cases the mechanical energy is then converted into electrical energy because of its greater versatility and adaptability as a form of energy.

Even though the ideal Rankine cycle is quite simple, a significant number of improvements can still be made to it in order to enhance the performance of the system and increase its energetic efficiency – reheating, regeneration, increasing or decreasing the pressure can all be considered, in order to make the most of a power plant.

In most cases, water is used as the working fluid because it is non-toxic, non-reactive, abundant, cost-effective, and displays good thermodynamic properties. However, using an organic fluid is also an option to help further increase the efficiency of the Rankine cycle or to harness medium temperature hot sources such as geothermal, biomass solar energy, or for waste heat recovery. In which case, this new cycle is known as an ORC, but even this can be further improved in many ways using reheaters and/or recuperators for instance. The use of new fluids also allows for greater flexibility, in that different fluids may be more suitable for specific applications, thus allowing them to reach their greatest possible efficiency. Hence, as discussed earlier, the selection of the right working fluid is crucial to efficient operation. To assist in this choice, organic fluids are divided into three families: wet-type fluids, dry-type fluids, and isentropic fluids, and currently a huge number of studies are focusing on the integration of ORC with existing systems so as to improve their overall efficiency.

Recent technological advances also allow the working fluid (water or organic fluid) to be used in supercritical conditions in order to improve the amount of work provided by the turbine(s) of a power plant.

In this respect, the Kalina cycle can be considered as the biggest step forward since the development of the Rankine steam cycles and ORCs. The technology presents a better energetic efficiency than steam cycles particularly for low-grade temperature applications such as geothermal and waste heat recovery.

The technology is relatively new; hence the capital expenditure necessary for a Kalina cycle-based power plant is, in most cases, higher than for a conventional system. However, as the Kalina cycle systems have a higher efficiency, their payback period is reduced, particularly for the latest second-generation cycles. It is also important to note that the Kalina cycles are a family of thermodynamic cycles and so a vast number of configurations exist, each one being suitable for a specific application. In most cases, a water–ammonia mixture is used as the working fluid in those

employing binary cycles. Indeed, this fluid offers interesting thermal performance; is compatible with standard materials and components; is ecological-friendly, abundant, and relatively inexpensive.

The reverse Kalina cycle is also a widely known thermodynamic cycle in that it is the absorption refrigeration cycle. This cycle uses an absorber and a generator instead of a compressor to carry out the suction and compression processes, meaning that almost no electricity is required to run the cycle. The future of Kalina cycles seems promising. An ever-increasing number of scientific studies are addressing the integration of this cycle in various systems: geothermal power plants, cement plants, concentrated solar power plants, and biomass power plants.

Now the Brayton cycle, although different to the Rankine cycle and its derivatives in that it is an open thermodynamic cycle, still has the same role to play as the closed power cycle – converting heat into mechanical energy – and the cycle efficiency can also be improved by using different technologies such as regeneration, reheating, and intercooling. The Brayton cycle can also use organic fluids as their working fluid (CO_2 in most cases) and sometimes these fluids too can operate under supercritical conditions with a further increase in efficiency.

But we are not just thinking about systems in isolation. Even if Rankine cycles and Brayton cycles are quite different, they can still be used together in combined cycles. In the CCGT plant, those two cycles are used together to reach a relatively high overall thermal efficiency (from 50% to 63%). So high, that the association of the Rankine cycle with the Brayton cycle is currently the most efficient way of producing electricity on a large scale. For example, the Chubu Electric Nishi-Nagoya power plant Block-1 in Japan is achieving a gross efficiency of 63.08%, and so is currently recognised as the world's most efficient combined cycle power plant.

References

1 Zhou, F., Joshi, S.N., Rhote-Vaney, R., and Dede, E.M. (2017). A review and future application of Rankine cycle to passenger vehicles for waste heat recovery. *Renewable Sustainable Energy Rev.* 75: 1008–1021. https://doi.org/10.1016/j.rser.2016.11.080.

2 Sattari, A. (2017). A novel design of a low Cost CSP using turbocharger as an expander. *J. Sol. Energy Res.* 2: 20–24.

3 Janie Ling-Chin, H.B.Z.M., Taylor, W., and Roskilly, A.P. (2019). Chapter 4: State-of-the-art technologies on low-grade heat recovery and utilization in industry. In: *Energy Conversion. Current Technologies and Future Trends*. IntechOpen https://doi.org/10.5772/intechopen.78701.

4 Sethi, A., Vera Becerra, E., and Yana Motta, S. (2016). Low GWP R134a replacements for small refrigeration (plug-in) applications. *Int. J. Refrig.* 66: 64–72. https://doi.org/10.1016/j.ijrefrig.2016.02.005.

5 Shang, R., Zhang, Y., Shi, W. et al. (2014). Fresh look and understanding on carnot cycle. *Energy Procedia* 61: 2898–2901. https://doi.org/10.1016/j.egypro.2014.12.213.

6 Xu, W., Deng, S., Su, W. et al. (2018). How to approach Carnot cycle via zeotropic working fluid: Research methodology and case study. *Energy* 144: 576–586. https://doi.org/10.1016/j.energy.2017.12.041.

7 Greitzer, E.M. (n.d.). 8.6 Enhancements of Rankine cycles.ZSSI.

8 Weston, K.C. (2000). *Fundamentals of Steam Power 2.1 Introduction*, 1e. University of Tulsa.

9 Riddoch, F. and Craenen, S. (n.d.). Cogeneration at the foundation of Europe's energy policy.

10 IBGE. (n.d.). Guide Cogénération.

11 Mat, N., Chee, I., Tan, W., and Yatim, A.H.M. (2018). A comprehensive review of cogeneration system in a microgrid: a perspective from architecture and operating system. *Renewable and Sustainable Energy Rev.* 81 (Part 2): 2236–2263. https://doi.org/10.1016/j.rser.2017.06.034.

12 Dabwan, Y.N. and Pei, G. (2020). A novel integrated solar gas turbine trigeneration system for production of power, heat and cooling: thermodynamic-economic-environmental analysis. *Renewable Energy* 152: 925–941. https://doi.org/10.1016/j.renene.2020.01.088.

13 Goncalv, E., Silva, D., Thibault, J. (2008). Cycles thermodynamiques des machines thermiques. Institut Polytechnique de Grenoble, 153.

14 Association WN. (n.d.). Advanced Nuclear Power Reactors | Generation III+ Nuclear Reactors.

15 Administration USEI. (n.d.). SAS Output.

16 Quoilin, S., Van Den, B.M., Declaye, S. et al. (2013). Techno-economic survey of organic rankine cycle (ORC) systems. *Renewable Sustainable Energy Rev.* 22: 168–186. https://doi.org/10.1016/j.rser.2013.01.028.

17 Al-Taha WH, Osman HA. Performance analysis of a steam power plant: a case study 2018. MATEC Web of Conferences, Volume 225, UPT-UMP-VIT Symposium on Energy Systems doi:https://doi.org/10.1051/matecconf/201822505023.

18 Inc AP. (n.d.). Economics and feasibility of rankine cycle improvements for coal fired power plants.

19 Minea, V. (2014). Power generation with ORC machines using low-grade waste heat or renewable energy. *Appl. Therm. Eng.* 69: 143–154. https://doi.org/10.1016/j.applthermaleng.2014.04.054.

20 Darvish, K., Aliehyaei, M., Atabi, F., and Rosen, M. (2015). Selection of optimum working fluid for organic Rankine cycles by exergy and exergy-economic analyses. *Sustainability* 7: 15362–15383. https://doi.org/10.3390/su71115362.

21 Abas, N., Kalair, A.R., Khan, N. et al. (2018). Natural and synthetic refrigerants, global warming: a review. *Renewable Sustainable Energy Rev.* 90: 557–569. https://doi.org/10.1016/j.rser.2018.03.099.

22 Nair, V. (2021). HFO refrigerants: a review of present status and future prospects. *Int. J. Refrig.* 122: 156–170. https://doi.org/10.1016/j.ijrefrig.2020.10.039.

23 Linde Group (2013). Safety Data Sheet – Heptafluorpropane (R227).

24 Linde Group (2014). Safety Data Sheet – Pentafluoropropane (R245fa).

25 Linde Group (2013). Safety Data Sheet – Isobutane (R600a).

26 Yang, H., Xu, C., Yang, B. et al. (2020). Performance analysis of an organic Rankine cycle system using evaporative condenser for sewage heat recovery in the petrochemical industry. *Energy Convers. Manage.* 205: 112402. https://doi.org/10.1016/j.enconman.2019.112402.

27 Baldasso, E., Andreasen, J.G., Mondejar, M.E. et al. (2019). Technical and economic feasibility of organic Rankine cycle-based waste heat recovery systems on feeder ships: impact of nitrogen oxides emission abatement technologies. *Energy Convers. Manage.* 183: 577–589. https://doi.org/10.1016/j.enconman.2018.12.114.

28 Yue, C., Tong, L., and Zhang, S. (2019). Thermal and economic analysis on vehicle energy supplying system based on waste heat recovery organic Rankine cycle. *Appl. Energy* 248: 241–255. https://doi.org/10.1016/j.apenergy.2019.04.081.

29 Sikarwar, S.S., Surywanshi, G.D., Patnaikuni, V.S. et al. (2020). Chemical looping combustion integrated organic Rankine cycled biomass-fired power plant – Energy and exergy analyses. *Renewable Energy* 155: 931–949. https://doi.org/10.1016/j.renene.2020.03.114.

30 Alvi, J.Z., Feng, Y., Wang, Q. et al. (2020). Modelling, simulation and comparison of phase change material storage based direct and indirect solar organic Rankine cycle systems. *Appl. Therm. Eng.* 170: 114780. https://doi.org/10.1016/j.applthermaleng.2019.114780.

31 Li, W., Lin, X., Cao, C. et al. (2018). Organic Rankine cycle-assisted ground source heat pump combisystem for space heating in cold regions. *Energy Convers. Manage.* 165: 195–205. https://doi.org/10.1016/j.enconman.2018.03.062.

32 Saghafifar, M., Omar, A., Mohammadi, K. et al. (2018). A review of unconventional bottoming cycles for waste heat recovery: Part I-Analysis, design, and optimization. *Energy Convers. Manag.* 198 https://doi.org/10.1016/j.enconman.2018.10.047.

33 Zhang, X., He, M., and Zhang, Y. (n.d.). A review of research on the Kalina cycle. *Renewable Sustainable Energy Rev.* 16 (7) https://doi.org/10.1016/j.rser.2012.05.040.

34 Globalgeothermal. (n.d.) Global Geothermal-Kalina Cycle application.

35 Schenker, S., Mccandless, D.W., Brophy, E., and Lewis, M.S. (1967). Studies on the intracerebral toxicity of ammonia. *J. Clin. Investig.* 46: 838–848.

36 Ambriz-Díaz, V.M., Rubio-Maya, C., Chávez, O. et al. (2021). Thermodynamic performance and economic feasibility of Kalina, Goswami and Organic Rankine Cycles coupled to a polygeneration plant using geothermal energy of low-grade temperature. *Energy Convers. Manag.* 243: 114362. https://doi.org/10.1016/j.enconman.2021.114362.

37 Global cement. (n.d.). Kalina bottoming cycle vs Rankine (ORC) in thermal power plant design.

38 Mirolli, M., Happ, K. (2012). Global CempPower Conference. FLSmidth & Co A/S.

39 Global cement. (2012). Kalina Cycle power systems in waste heat recovery applications.

40 Omar, A., Saghafifar, M., Mohammadi, K. et al. (2018). A review of unconventional bottoming cycles for waste heat recovery: Part II-Applications. *Energy Convers. Manage.* https://doi.org/10.1016/j.enconman.2018.10.088.

41 Kalinapower. (n.d.). Kalina – Electricity from heat.

42 Blanco, M. and Lourdes, R.S. (2017). *Advances in Concentrating Solar Thermal Research and Technology*. Google Livres.

43 Nasruddin, U.R., Rifaldi, M., and Noor, A. (2009). Energy and exergy analysis of kalina cycle system (KCS) 34 with mass fraction ammonia-water mixture variation. *J. Mech. Sci. Technol.* 23: 1871–1876. https://doi.org/10.1007/s12206-009-0617-8.

44 Wang, E. and Yu, Z. (2016). A numerical analysis of a composition-adjustable Kalina cycle power plant for power generation from low-temperature geothermal sources. *Appl. Energy* 180: 834–848. https://doi.org/10.1016/j.apenergy.2016.08.032.

45 Kalex Systems LLC. (2009). Kalex Kalina Cycle Power Systems for Geothermal Applications.

46 Renz, M., Engelhard, M., Zander, M. (2006). The New Generation Kalina Cycle Contribution to the conference "*Electricity Generation from Enhanced Geothermal Systems*."

47 Kalex Systems LLC. (2009). Kalex Kalina Cycle Power Systems for Geothermal Applications.

48 Lcak HM, Ark M, Irolli M, Hjartarson H, Húsavíkur O. (2002). Notes from the North: A Report on the Debut Year of the 2 MW Kalina Cycle ® Geothermal Power Plant in Húsavík, Iceland.

49 G-u M. (2010). *The Geothermal Power Plant Bruchsal*.

50 Kalina Power. (2016). Introduction to Kalina Cycle®. Kalina Power Limited.

51 Huang, K., Marthinsen, K., Zhao, Q., and Logé, R. (2018). The double-edge effect of second-phase particles on the recrystallization behaviour and associated mechanical properties of metallic materials. *Prog. Mater. Sci.* 92: 284–359. https://doi.org/10.1016/j.pmatsci.2017.10.004.